HHS Public Access

Author manuscript

Toxicol Appl Pharmacol. Author manuscript; available in PMC 2018 March 01.

Published in final edited form as:

Toxicol Appl Pharmacol. 2017 March 01; 318: 58–68. doi:10.1016/j.taap.2017.01.012.

Phagolysosome Acidification is Required for Silica and Engineered Nanoparticle-induced Lysosome Membrane Permeabilization and Resultant NLRP3 Inflammasome Activity

Forrest Jessop[*], **Raymond F. Hamilton Jr**[*], **Joseph F. Rhoderick**[*], **Paige Fletcher**[*], and **Andrij Holian**[*,1]

[*]Center for Environmental Health Sciences, Department of Biomedical and Pharmaceutical Sciences, University of Montana, Missoula, Montana

Abstract

NLRP3 inflammasome activation occurs in response to hazardous particle exposures and is critical for the development of particle-induced lung disease. Mechanisms of Lysosome Membrane Permeabilization (LMP), a central pathway for activation of the NLRP3 inflammasome by inhaled particles, are not fully understood. We demonstrate that the lysosomal vATPases inhibitor Bafilomycin A1 blocked LMP *in vitro* and *ex vivo* in primary murine macrophages following exposure to silica, multi-walled carbon nanotubes, and titanium nanobelts. Bafilomycin A1 treatment of particle-exposed macrophages also resulted in decreased active cathepsin L in the cytosol, a surrogate measure for leaked cathepsin B, which was associated with less NLRP3 inflammasome activity. Silica-induced LMP was partially dependent upon lysosomal cathepsins B and L, whereas nanoparticle-induced LMP occurred independent of cathepsin activity. Furthermore, inhibition of lysosomal cathepsin activity with CA-074-Me decreased the release of High Mobility Group Box 1. Together, these data support the notion that lysosome acidification is a prerequisite for particle-induced LMP, and the resultant leak of lysosome cathepsins is a primary regulator of ongoing NLRP3 inflammasome activity and release of HMGB1.

Graphical Abstract

[1]To whom correspondence should be addressed: Prof. Andrij Holian, Center for Environmental Health Sciences, University of Montana, 32 Campus Dr, Missoula, Montana 59812, Telephone: (406) 243-4478 FAX: (406) 243-2807; andrij.holian@umontana.edu.

Conflicts of Interest

The authors declare that they have no conflicts of interests with the contents of this article.

Author Contributions

FJ designed and carried out both the *in vitro*, and 7 d *in vivo* and *ex vivo* studies in the manuscript, and performed statistical analysis. FJ wrote the first draft of the manuscript. RFH performed the *ex vivo* studies and cytokine analysis on AM isolated 56 d after silica exposure. RFH helped with the statistical analysis. JFR performed mRNA quantification by RT-PCR for the 7 d studies and assisted with BMdM *in vitro* studies. PF assisted FJ with the caspase-1 null mouse studies. AH assisted FJ in overall study design and coordination. All authors helped further draft the manuscript and approved the final manuscript.

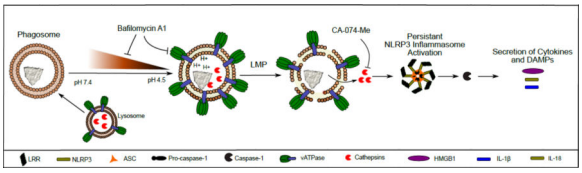

Keywords

NLRP3 inflammasome; MWCNT; TNB; Silica; Lysosome Membrane Permeabilization

INTRODUCTION

Silica was one of the first environmental particles identified to activate the NLRP3 inflammasome (Dostert *et al.*, 2008; Hornung *et al.*, 2008). It is now known that many particles, exogenous and endogenous, environmental and engineered, of many sizes and shapes, are activators of the NLRP3 inflammasome. Therefore, inflammasome activity and associated signaling pathways are common targets for next generation therapeutics. Particle-induced NLRP3 inflammasome assembly results in activation of caspase-1, which cleaves pro-IL-1β and pro-IL-18 to their active forms prior to secretion. These cytokines play central roles in the development of chronic inflammatory lung diseases (Netea *et al.*, 2015). With the rapidly expanding market of engineered nanomaterial (ENM), there is cause for concern as many of these particles could potentially cause chronic inflammatory lung disease through mechanisms similar to those observed with silica exposure.

Mechanisms by which particles cause NLRP3 inflammasome activation are not fully understood. In the lung, inhaled particles are phagocytosed by alveolar macrophages (AM). Within AM, the phagosome containing particle(s) fuses with lysosomes in order to attempt to degrade the particle. Consistent with this notion, others and our group have observed silica and ENM, including Multi-walled Carbon Nanotubes (MWCNT) and Titanium Nanobelts (TNB), within phagolysosomal compartments in AM following exposure (Gilberti *et al.*, 2008; Hamilton *et al.*, 2009; Hamilton *et al.*, 2013; Hamilton *et al.*, 2014). Silica, MWCNT, TNB and numerous other nanomaterials are resistant to lysosomal degradation, and consequently, downstream consequences are not fully understood. Phagocytized silica particles have been reported to cause Lysosome Membrane Permeabilization (LMP) contributing to NLRP3 inflammasome activation and cell death (Cassel *et al.*, 2008; Hornung *et al.*, 2008). Likewise, prior studies report qualitative data consistent with MWCNT and TNB-induced LMP, which resulted in NLRP3 inflammasome activation and toxicity in macrophages *in vitro* (Hamilton *et al.*, 2009; Sohaebuddin *et al.*, 2010; Hamilton *et al.*, 2012; Meunier *et al.*, 2012). However, these studies do not address what lysosome mediated events support particle-induced LMP. Consequently, the mechanisms responsible for particle-induced LMP remain to be determined.

Active lysosomal proteases and low pH are reported to be necessary for removal of protein coronas on nanomaterials (Wang *et al.*, 2013), which may allow for direct particle-membrane interactions resulting in LMP. Critical to phagolysosomal acidification are recruitment and activation of vATPases. Furthermore, optimal activation of lysosomal

proteases is contingent on a low pH environment (Lennon-Dumenil *et al.*, 2002). When leaked from the lysosome, active cathepsin B facilitates NLRP3 inflammasome assembly (Hornung *et al.*, 2008). Phagolysosome acidification has been reported to play a role in LMP following treatment with Leu-Leu-OMe (Hornung *et al.*, 2008), likely through decreased Dipeptide Peptidase I (cathepsin C) activity, which processes the agent to its active form (Jacobson *et al.*, 2013). Phagolysosome acidification is suspected to play a role in LMP with silica exposure due to the inhibitory activity of Bafilomycin A1 on downstream NLRP3 inflammasome activity (Hornung *et al.*, 2008). Whether Bafilomycin A1 inhibition of NLRP3 inflammasome activity with silica exposure is due to direct inhibition of LMP, or inhibition of the activation of cathepsin B, is not known. Also, whether other NLRP3 inflammasome activating nanomaterials, including MWCNT and TNB, cause LMP similar to silica has not been tested. Therefore, the contribution of phagolysosome acidification to silica and nanoparticle-induced LMP remains to be determined. Some reports suggest that active cathepsin B may directly participate in causing LMP (Werneburg *et al.*, 2002; Taha *et al.*, 2005; Moles *et al.*, 2012; Brojatsch *et al.*, 2014). However, the role of cathepsin B in causing LMP with particle exposure has not been elucidated.

The objective of this study was to determine mechanisms contributing to silica-induced LMP, including the role of phagolysosome acidification and cathepsins, and if they are shared by other NLRP3 inflammasome activating nanomaterials including MWCNT and TNB. We hypothesized that LMP would be dependent upon lysosome acidification, and LMP would drive NLRP3 inflammasome activity persistence *in vivo*. The findings from this work provide new incite into central mechanisms through which hazardous particles cause LMP and the role of LMP in ongoing inflammation.

EXPERIMENTAL PROCEDURES

Particle Preparation

Our laboratory and others have extensively characterized the physiochemical properties, dispersion, and associated lung pathology of silica, MWCNT, TNB, and TNS used in these experiments in prior studies (Hamilton et al., 2006; Hamilton *et al.*, 2009; Beamer *et al.*, 2010; Hamilton *et al.*, 2012; Xia et al., 2013; Girtsman *et al.*, 2014) (see Supplemental Table 1). LPS levels were determined to be negligible by the Limulus amebocyte lysate assay (Cambrex, Walkersville, MD, USA). Acid washed crystalline silica (Min-U-Sil-5, Pennsylvania Glass Sand Corp, Pittsburgh, PA, USA) was prepared fresh in phosphate-buffered saline (PBS, pH 7.4) and sonicated (550 watts @ 20 kHz) for 1 min in a cup-horn sonicator (Misonix, Inc. Farmingdale, NY, USA) prior to use. MWCNT (Sun Innovations, Inc., Fremont CA, USA) was prepared fresh in dispersion medium (DM, 0.6 mg/mL mouse serum albumin (Sigma-Aldrich, Saint Louis, MO, USA) and 0.01 mg/mL 1,2-dipalmitoyl-sn-glycero-3-phosphocholine (Sigma-Aldrich) in PBS) and sonicated (550 watts @ 20 kHz) for 1 min in a cup-horn sonicator (Porter *et al.*, 2013). Dr. Nigel Walker and Brad Collins at the National Toxicology Program (NTP) at the National Institute of Environmental Health Sciences (NIEHS) provided the MWCNT. TNB and TNS were prepared and provided by Dr. Nianqiang Wu at West Virginia University (Morgantown, WV, USA) (Hamilton *et al.*, 2009;

Porter *et al.*, 2013). TNB and TNS were suspended in PBS using a stir bar for 1 hr due to potential fracture by sonication (Xia *et al.*, 2013).

Mice

Both male and female C57Bl/6 and caspase-1 null mice (Jackson Laboratories, Bar Harbor, ME, USA) were used in equal numbers for all studies. Animals were housed in micro-isolators in a specific pathogen-free facility under a 12:12-hr light-dark cycle. Food, bedding, and cages were sterilized by autoclaving. Mice were used between 8–12 wk of age. The University of Montana Institutional Animal Care and Use Committee (Missoula, MT, USA) approved all procedures performed on the animals.

Bone Marrow derived Macrophages

BMdM were obtained as described previously [30]. Briefly, wild-type C57Bl/6 were sacrificed and bone marrow was flushed from the isolated femur and tibia with media. Cells were then incubated in T75 culture flasks (20 mL RPMI + 10% FCS) overnight for stromal cell elimination. Aspirated cells were transferred to new T75 flasks in (15×10^6 cells/flask in 20 mL RPMI + 10% FCS) and 40 μL macrophage colony stimulating factor (M-CSF) added (10 ng/mL stock, R&D Systems). Cultures continued for 7–10 days with re-feeding and M-CSF spiking every 3–4 days.

Assessment of NLRP3 inflammasome activity in vitro

BMdM were plated in a 96-well plate (1×10^5 cells/well) and exposed to particles and LPS (20 ng/mL) for inflammasome priming. Cells were treated with/without the cathepsin inhibitor CA-074-Me (10 μM, Peptides International, Louisville, KY, USA) or Bafilomycin A1 (100 nM, EnzoLife Sciences, Farmingdale, NY, USA) and cell supernatants were collected after 24 hours. Cell supernatants were assessed for IL-1β by ELISA (R&D Systems, Minneapolis, MN, USA). IL-18 was measured by an in-house ELISA previously described (Hamilton *et al.*, 2014).

In vivo and ex vivo assessment of NLRP3 inflammasome activity

Mice were anaesthetized using isoflurane inhalation and then exposed to silica (40 mg/kg or 1 mg/25 g mouse) or MWCNT, TNB or TNS (2 mg/kg or 50 μg/25 g mouse), by oropharyngeal aspiration (Lacher *et al.*, 2010). The doses used for these studies were selected based on their inflammatory activity established in prior work (Hamilton *et al.*, 2009; Beamer *et al.*, 2010; Hamilton *et al.*, 2012; Girtsman *et al.*, 2014). Mice were lavaged after 7 d for analysis of inflammation and LMP. For chronic studies, mice were instilled once a week with silica for 4 consecutive weeks and sacrificed 56 d following the first instillation (Beamer *et al.*, 2010). AM were isolated from the lavage fluid from both the early (7 d) and chronic time points (56 d) and cultured *ex vivo* in RPMI + 10% FCS for 24 hr with or without LPS (20 ng/mL) and the cathepsin B inhibitor CA-074-Me (10 μM) and/or Bafilomycin A1 (100 nM). Cell supernatants and cell free lavage fluid were assessed for IL-1β and IL-18 by ELISA as previously described. HMGB1 was measured by ELISA using commercially available antibodies (R&D Systems; EMD Millipore, Billerica, MA, USA; Santa-Cruz Biotech, Dallas, TX, USA) as previously described (Jessop and Holian,

2015). Whole Lung lavage fluid was also assessed for LDH activity (Promega, Madison, WI, USA) and protein content using the BCA assay (Thermo Fisher Scientific, Waltham, MA, USA).

Lysosome Membrane Permeabilization (LMP) assay

LMP was assessed using methods modified from Aits et al (Aits *et al.*, 2015). Isolated AM were plated in a 96 well plate at 1×10^5 cells per well and allowed to adhere for 2 hours. For BMdM, cells were plated at 2×10^5 cells per well in a 24 well plate. Cells were washed twice with PBS to remove dead cells and debris. AM or BMdM were then incubated with 100 μL (for 96 well format) or 200 μL (for 24 well format) of cytosol extraction buffer (250 mM sucrose, 20 mM Hepes, 10 mM KCl, 1.5 mM $MgCl_2$, 1 mM EDTA, 1 mM EGTA, 0.5 mM pefabloc (Sigma-Aldrich), pH 7.5 + digitonin (Sigma-Aldrich)) for 15 min on ice with rocking. The concentration of digitonin for optimal extraction of the cytosolic fraction was obtained by titration (BMdM = 12.5 μg/mL; AM = 17.5 μg/mL). 50 μL of extracted cytosol was then added to 50 μL of cathepsin reaction buffer (50 mM sodium acetate, 4 mM EDTA, pH 6.0 + fresh 0.5 mM pefabloc, 8 mM DTT, 50 μM cathepsin L substrate (Z-Phe-Arg-AFC, EnzoLife Sciences)) and read using a plate reader (25 min; 45 sec intervals; 400 nm excitation; 489 nm emission). β-*N*-acetylglucosaminidase (NAG) activity was measured by adding 30 μL cytosolic extract to 100 μL of NAG reaction buffer (0.2 M sodium citrate, pH 4.5 with 300 μg/mL 4-methylumbelliferyl-2-acetamido-2-deoxy-β-D-glucopyranoside (Sigma-Aldrich)) and assessed on a plate reader (20 min; 45s intervals; 356 nm excitation; 444 nm emission). LDH activity was assessed following manufacture's instructions (Promega). Extracted cytosolic LDH activity was used as an internal control to which cytosolic cathepsin L or NAG activities were normalized. Cytosolic extract enzyme activities were calculated as a percent of total cell lysate activity in which 200 μg/mL of digitonin was used to completely lyse the cell.

Extracellular Cathepsin Activity Assay

Extracellular cathepsin activity was assessed as previously described by our laboratory (Sager *et al.*, 2014). Briefly, 2 μg Z-LR-AMC (specific to cathepsin B, cathepsin L and cathepsin V; R&D systems) in PBS was added to 50 μL of whole lung lavage fluid in a total reaction volume of 150 μL. The assays were incubated at 37°C for 1 h then fluorescence was measured using a plate reader at 380 nm excitation and 460 nm emission.

RNA preparation and RT-PCR

Isolated AM (4 mice pooled for each N) from mice 7 d following PBS or silica exposure were lysed and total RNA isolated in Trizol (Thermo Fisher Scientific). The RNA Integrity Number (RIN) and total RNA concentration was confirmed using the RNA 6000 Nano Kit (Agilent Technologies, Santa Clara, CA, USA) and Agilent Bioanalyzer 2000. Prior to cDNA synthesis, 100 ng of total RNA was treated with 1–2 U of DNAse I (Quanta Biosciences, Gaithersburg, MD, USA). All RNA samples were reverse transcribed using iScript Reverse Transcription Supermix (BioRad, Hercules, CA, USA) in accordance with the manufacturer's protocol. PrimeTime qPCR primers to Caspase-1 (*Casp1*, Prime Time Assay Mm.PT.58.13005595), IL-1β (*Il-1b*, Mm.PT.58.42940223), NLRP3 *(Nlrp3*, Mm.PT. 58.42443451), ASC (*Pycard*, Mm.PT.56a.42872867), and reference genes *Adck1* (Mm.PT.

56a.41787370) and *Pigo* (Mm.PT.58.6147472) were used for RT-PCR reactions (IDT, Coralville, IA, USA). Efficiency for PrimeTime primers were established via standard curve analysis of at least two biological replicates using cDNA synthesized from AM or genomic DNA isolated from murine lung tissue respectively. Efficiencies for all primer pairs used in PCR analysis >89%. All signals were normalized to *Adck1* and *Pigo* and relative expression levels determined using the REST 2009 v2.0.13 software suite (Qiagen, Valencia, CA, USA).

Western Blot

Isolated cells obtained from lung lavage fluid were lysed directly in RIPA buffer containing HALT™ protease inhibitors (Life Technologies, Carlsbad, CA, USA). Whole lung lavage cells from 3 mice were pooled for each *N*. Lysates were run on 4–12% Bis-Tris SDS-PAGE gels. Anti-NLRP3 antibodies were obtained from R&D Systems. Anti-ASC, Anti-caspase-1, and anti-pro-IL-1β antibodies were obtained from Novus Biologicals (Littleton, CO, USA). The secondary antibodies were donkey anti-rabbit conjugated to horseradish peroxidase (BioLegend, San Diego, CA, USA).

Immunofluorescences Detection of Cathepsin B and Lysotracker™ Red

Cathepsin B and lysosomes were measured using a CompuCyte iCys Laser Scanning Cytometer (LSC, Westwood, MA, USA). Briefly isolated AM were seeded in triplicate in a 96-well plate with a glass coverslip bottom (MatTeck Corp. Ashland, MA, USA) at 1×10^5 cells/well. After 1 hour, non-adherent cells were removed by gentle washing once with PBS. Cells were then stained using the Magic Red™ Cathepsin B Detection Kit (ImmunoChemistry Technologies, Bloomington, MN, USA) or LysoTracker Red DND-99 dye (Life Technologies) and counter-stained with Molecular Probes HCS NuclearMask Blue stain (Life Technologies) according to manufacture's instructions. The cathepsin B signal or Lysotracker Red signal was detected using a 561 nm laser as the excitation source and a PMT detector with a 600/50 nm bandpass filter. The nuclear staining was excited with a 405 nm laser and detected with a 440/30 nm bandpass filter/PMT set. Individual passes of the 561 nm and 405 nm lasers were used to avoid any spectral overlap of the "blue" and "red" fluorescent signals. A threshold of "blue" fluorescence was set such that the software draws a contour around the nucleus of the cell. The contour is then expanded by 20 pixels to include the cytoplasm of the cell. Each cell (defined by nuclear staining) is plotted on a histogram showing Red Mean Fluorescent Intensity (MFI). Regions were defined within each well of the 96-well plate to include approximately 1500 cells to achieve sufficient sample representation.

Statistical analysis

Statistical analyses involved comparison of means using a one- or two-way ANOVA followed by a Bonferroni's test to compensate for increased type I error. Unpaired t test was utilized for analysis of Western Blots or other data sets that included simple comparisons between two groups. All probabilities were two-tailed. Statistical power was > 0.8 to determine sample size. Statistical significance was defined as a probability of type I error occurring at < 5% ($P<0.05$). The minimum number of experimental replications was 3. Graphics and analyses were performed on PRISM 5.0 and PRISM 6.0.

RESULTS

Crystalline Silica and ENM induce LMP in macrophages

Silica has been reported to cause LMP *in vitro* (Hornung *et al.*, 2008), and LMP has been proposed, but not directly quantified with the other ENM, including those used in the current studies (Hamilton *et al.*, 2009; Palomaki *et al.*, 2011; Hamilton *et al.*, 2012). To assess LMP, we adapted recently reported methods that use digitonin extraction of the cytosol in order to measure leaked lysosomal cathepsin L and/or *N*-acetyl-β-D-glucosaminidase (NAG) activity (Supplementary Figure 1) (Aits *et al.*, 2015). For these studies, we utilized BMdM to help determine LMP *in vitro*. BMdM were exposed to increasing doses of silica, MWCNT, TNB, and TNS and LMP quantified at 4 hr. We also quantified LMP over an 18 hr time-course. All particles were able to induce LMP with increasing dose (Figure 1A), however, the kinetics of LMP-induction for each particle differed. While TNS caused LMP, it was significantly less than silica and TNB. LMP following silica exposure peaked at 4 hours, while LMP increased over time with ENM exposures (Figure 1B). These findings reveal important differences between the kinetics of silica and ENM-induced LMP within the first 18 hr of exposure *in vitro*. However, exposure to all particles eventually resulted in significant LMP by 18 hr.

Phagolysosome acidification is necessary for silica and ENM-induced LMP

How bioactive particles including silica, MWCNT, and TNB cause LMP and whether LMP is dependent on phagolysosome acidification has not been determined. Therefore, we exposed BMdM to these particles with or without Bafilomycin A1 treatment, which specifically inhibits vATPases responsible for lysosome acidification (Yoshimori *et al.*, 1991). We then measured LMP after 4 hr and resultant downstream NLRP3 inflammasome activity (extracellular IL-18 and IL-1β levels) after 24 hr. Bafilomycin A1 inhibited LMP, as indicated by decreased cytosolic cathepsin L activity, with all particle exposures (Figure 2A). However, since Bafilomycin A1 can prevent cathepsin maturation possibly interfering with the assay, we measured leaked NAG as a second indicator of LMP. NAG activity is not necessarily dependent upon a lower lysosomal pH and has a longer half-life in the cytosol following LMP (Aits *et al.*, 2015). NAG activity in the cytosolic fraction was significantly decreased with Bafilomycin A1 treatment for all particles (Figure 2B, 2C), confirming the necessity of phagolysosome acidification in particle-induced LMP. The observation that LMP was decreased with Bafilomycin A1 treatment was not due to decreased particle uptake (data not shown). Finally, as expected, inhibition of LMP with Bafilomycin A1 decreased NLRP3 inflammasome activity including the release of IL-18 and IL-1β, for all particles tested (Figure 2D, 2E).

Cathepsin B and L are not necessary for silica and ENM-induced LMP

While most studies agree that cathepsin B is important in activating the NLRP3 inflammasome after LMP, there are reports suggesting a direct role for cathepsin B and possibly other cathepsins in facilitating LMP with cholesterol crystals, adjuvants and sphingosine (Werneburg *et al.*, 2002; Taha *et al.*, 2005; Duewell *et al.*, 2010; Jacobson *et al.*, 2013). This relationship has not been determined for silica and ENM exposure. Therefore, to determine if cathepsin B was directly involved in LMP, we exposed BMdM to silica,

MWCNT, TNB and TNS with or without CA-074-Me treatment and assessed LMP after 4 hr. CA-074-Me has been shown to have high specificity towards cathepsin B and partial specificity to cathepsin L (Buttle *et al.*, 1992), and CA-074-Me inhibition of cathepsin L is increased in reducing conditions (Steverding, 2011).

Consequently, measuring active cytosolic cathepsin L activity as an indicator of LMP may be problematic with CA-074-Me treatment. Indeed, we found that CA-074-Me treatment did greatly decrease cathepsin L activity in the cytosolic fraction of particle-exposed macrophages (Figure 2A). However, CA-074-Me did not inhibit cathepsin L when added in situ to cytosolic extracts, supporting the notion that CA-074-Me may be inhibiting cathepsin L under reducing conditions *in vitro* (Supplementary Figure 2). When leaked NAG was measured as the primary indicator of LMP, we found that CA-074-Me treatment partially reduced cytosolic NAG activity with silica exposure (Figure 2B), but did not reduce cytosolic NAG activity with ENM exposures (Figure 2C). These findings support the notion that the nanoparticles used in these studies cause LMP independent of cathepsin B and L. However, cathepsin B and or cathepsin L may have marginal or indirect roles in LMP with silica exposure.

Finally, we measured IL-18 and IL-1β production with particle exposure with or without CA-074-Me treatment at 24 hr to confirm that active cathepsin B/L has an integral role in NLRP3 inflammasome activation downstream of LMP. Extracellular IL-18 and IL-1β levels were significantly reduced with CA-074-Me treatment for all particles used (Figure 2D, 2E). These data provide further support for the importance of cathepsin B, and possibly cathepsin L, in activating the NLRP3 inflammasome after LMP *in vitro*.

Increased NLRP3 inflammasome activity associates with altered lysosomal staining and cathepsin activity in vivo

Our next objective was to assess the relationship between LMP and NLRP3 inflammasome activity *in vivo*. We hypothesized that particle exposure would result in ongoing NLRP3 inflammasome activity and altered lysosomal staining in AM, consistent with ongoing LMP. For these studies we tested silica as a representative particle, and measured relevant indicators of inflammation in C57Bl/6 mice at 7 d. Silica-exposed C57Bl/6 mice had significantly elevated total cell counts (Figure 3A), and exhibited increased levels of IL-1β, IL-18, and the alarmin HMGB1 in the lung lavage fluid (Figure 3B, 3C, 3D). Total protein levels and extracellular LDH activity were increased as well in silica-exposed C57BL/6 mice, supportive of ongoing inflammation and cell death (Supplemental Figure 3). Consistent with increased cytokine and alarmin production, we observed elevated NLRP3 inflammasome protein components NLRP3, ASC, and pro-caspase-1 1 in isolated AM (Figure 3E). mRNA levels for NLRP3 (*Nlrp3*), ASC (*Pycard*), and pro-IL-1β (*Il-1b*) were significantly increased as well (Figure 3F).

Since no active caspase-1 fragments were observed in our unprimed AM (Figure 3F), we utilized caspase-1 null mice to confirm that the observed inflammation was dependent on inflammasome activation. As predicted, total cell counts, IL-18, IL-1β, and HMGB1 were significantly reduced in silica-exposed caspase-1 null mice compared to C57Bl/6 controls (Figure 3A, 3B, 3C, 3D). Together, these results support the notion of ongoing NLRP3

inflammasome activity with silica exposure. Based on increased cellularity (Supplemental Figure 4) and pathology at 7 d reported in prior studies (Solano-Lopez *et al.*, 2006; Beamer *et al.*, 2010; Hamilton *et al.*, 2012; Porter *et al.*, 2013), we would expect similar findings with MWCNT and TNB exposures.

We next tested whether increased NLRP3 inflammasome activity correlated with altered lysosome staining and lysosomal cathepsin activity. Elevated extracellular cathepsin activity can be a consequence of lysosome disruption and associated cell death (Hughes *et al.*, 2016). We observed greater extracellular cathepsins (L, B, and/or V) activity in the lavage fluid of silica-exposed mice at 7 d (Figure 4A). Furthermore, silica exposure was also associated with increased intracellular cathepsin B activity (Figure 4B, 4C), consistent with altered lysosome state and ongoing NLRP3 inflammasome activity in macrophages. It is possible that LMP can result in the loss of intact lysosomes (Hornung *et al.*, 2008). AM isolated 7 d following exposure to silica had a lower mean fluorescence intensity (MFI) of Lysotracker™ Red staining compared to PBS control when assessed by laser scanning cytometry (Figure 4C). Evaluation of histograms (MFI of total cells counted) revealed that silica exposure caused the formation of two distinct cell populations based on MFI (Figure 4D). Together, these data support the notion that silica exposure causes NLRP3 inflammasome persistence at 7 d in AM *in vivo*, correlating with an altered lysosome staining and cathepsin B activity.

Silica and MWCNT exposure results in LMP in vivo

Direct evidence of LMP *in vivo* is sparse, let alone in models of particle exposure (Appelqvist *et al.*, 2013). Our data showing an altered lysosomal-macrophage staining with silica exposure may point to ongoing LMP *in vivo*. To assess LMP *in vivo* we exposed C57Bl/6 mice to silica. After 7 d we isolated the AM and extracted the cytosolic fraction in order to quantify LMP. Cathepsin L activity was significantly increased in the cytosol of AM from silica-exposed mice compared to PBS-treated mice, confirming LMP *in vivo* (Figure 5A). NAG activity was significantly increased as well (Figure 5B). Similarly, increased cytosolic NAG confirmed ongoing LMP with MWCNT exposure, and NAG increased, though not significantly, with TNB exposure (Figure 5C and 5D, NAG data only shown). Together, these data support ongoing LMP at 7 d following silica and ENM exposure.

We previously demonstrated that LMP was inhibited *in vitro* with Bafilomycin A1 (Figure 2A, 2B, 2C), highlighting a critical role for lysosome acidification in particle-induced LMP. CA-074-Me had partial activity in reducing LMP with silica exposure, but did not inhibit nanoparticle-induced LMP, suggesting LMP can occur independent of cathepsin B and or L activation (Figure 2B, C). To confirm the role of lysosome acidification and cathepsins in LMP *in vivo*, we treated AM isolated from silica and MWCNT-exposed mice (7 d) *ex vivo* with Bafilomycin A1 or CA-074-Me. Consistent with our *in vitro* results, Bafilomycin A1 significantly reduced LMP, as measured by cytosolic cathepsin and NAG levels, with silica exposure (Figure 5A, 5B). A similar response was observed with ENM exposure, though the decrease was not statistically significant (Figure 5C, 5D). Together, these findings support a role for lysosome acidification in ongoing LMP *in vivo* with exposure to these hazardous particles.

Similar to findings from the *in vitro* studies highlighted in Figure 2, CA-074-Me treatment partially reduced LMP in isolated AM from silica-exposed mice (Figure 5A, 5B). However, CA-074-Me did not decrease LMP with MWCNT exposure, and resulted in a nonsignificant decrease with TNB exposure (Figure 5C, 5D). CA-074-Me treatment decreased active cathepsin L with all treatment groups, consistent with our *in vitro* findings.

Persistent NLRP3 inflammasome activity is dependent upon LMP and cathepsin B

Our data supports the notion that NLRP3 inflammasome is active 7 d following silica and MWCNT exposure *in vivo* (Figure 3), and LMP can be blocked *ex vivo* with Bafilomycin A1 treatment (Figure 5). Consequently, we hypothesized that inhibition of phagolysosome acidification and/or active cathepsin B in AM isolated from particle-exposed mice would decrease NLRP3 inflammasome cytokines and HMGB1. To test this, we isolated AM from C57BL/6 mice 7 d after silica exposure and cultured them *ex vivo* with or without LPS (for inflammasome priming) and Bafilomycin A1 or CA-074-Me treatment, then measured secretion of IL-1β and IL-18. AM from silica exposed mice secreted significantly greater amounts of IL-1β and IL-18 than AM from PBS-exposed mice (Figure 6A, 6B). Bafilomycin A1 and CA-074-Me treatment significantly reduced IL-1β and IL-18 production *ex vivo* from AM in the silica-exposed groups (Figure 6A, 6B). CA-074-Me treatment also decreased HMGB1 secretion from silica-exposed AM, demonstrating a role for cathepsins in regulating the secretion of an alarmin that is not catalytically processed by the NLRP3 inflammasome (Figure 6C). Bafilomycin A1 treatment did not decrease HMGB1 release from AM *ex vivo* (data not shown), possibly due to increased cytotoxicity (Supplemental Figure 5). Conversely, CA-074-Me treatment of AM *ex vivo* significantly reduced LDH release, suggesting reduced cell death correlating with less HMGB1 release.

Next, we utilized a model of chronic lung disease previously established with silica (Beamer *et al.*, 2010) to test if NLRP3 inflammasome activity could be mitigated with CA-074-Me treatment in isolated AM. Since Bafilomycin A1 also inhibits activity of cathepsins (Figure 2), CA-074-Me was utilized in these studies to test the critical pathway following LMP that drives NLRP3 inflammasome activity. As predicted, IL-1β and IL-18 were significantly decreased with CA-074-Me treatment of AM isolated from mice with chronic lung disease (Figure 5C, 5D). Together, these data support persistent NLRP3 inflammasome activity in AM with silica exposure is dependent on upon active cathepsin B and or L, which are tightly regulated by lysosomal acidification.

Next, we repeated the 7 d *in vivo* exposures using MWCNT, TNB, and TNS in order to test if responses to CA-074-Me treatment were similar to those observed with silica exposure. CA-074-Me treatment significantly reduced IL-1β from AM isolated from MWCNT and TNB-exposed C57Bl/6 mice (Figure 6F). Furthermore, HMGB1 was significantly reduced with CA-074-Me treatment with TNB exposure (Figure 6G). Similar to results following silica exposure, these studies support a significant role for active cathepsins in driving persistent NLRP3 inflammasome activity with MWCNT and TNB exposure, and are consistent with ongoing LMP.

DISCUSSION

Compromised lysosome integrity is an emerging paradigm with environmental particle and ENM exposure, and this includes the potential for particles to cause LMP (Stern *et al.*, 2012). Lysosome dysfunction has been implicated in a number of chronic inflammatory diseases (Appelqvist *et al.*, 2013). Mechanisms by which silica and nanomaterial exposure results in LMP remain unclear, and advancement in this field has been complicated by difficulties in directly assessing LMP. Evaluation of LMP with particle exposure primarily has been done using acidotropic dyes or immunofluorescent staining to assess co-localization of lysosomal enzymes (Stern *et al.*, 2012). These assays can be difficult to interpret, since dye trapping and diffusion can be influence by lysosome number and relative acidification (Boya and Kroemer, 2008). Many nanomaterials, such as MWCNT and TNB, could also interfere with these fluorescent assays, especially at higher doses, further complicating assessment of LMP. Additionally, inhibitors that target lysosome acidification, such as Bafilomycin A1, can also affect the fluorescence of acidotropic dyes, influencing interpretation of mechanistic studies. In this study, we utilized methods adapted from Aits et al., which rely on the saponic qualities of digitionin for selective extraction of the cellular cytosolic fraction (Aits *et al.*, 2015), allowing for direct quantification of LMP in primary macrophages following particle exposure. Furthermore, these methods allowed for a more direct investigation of the role of lysosomal acidification in particle-induced LMP. The novel findings of this work are that LMP, following exposure to both silica and the specific ENM used in these studies, is dependent upon lysosome acidification *in vitro* and *in vivo*. Furthermore, following LMP, cathepsins are the primary signal regulating NLRP3 inflammasome activity. Furthermore, lysosomal cathepsins B or L, may play a marginal role in facilitating LMP with silica exposure, but did not appear to participate in LMP with ENM exposure. Additionally, our studies provide new evidence for cathepsin B/L regulation of the secretion of the alarmin HMGB1 with particle exposure.

Lysosome acidification has been reported to be necessary for LMP following Leu-Leu-O-Me exposure (Hornung *et al.*, 2008). However, inhibition of lysosome acidification by Bafilomycin A1 may also impair cathepsin maturation, including the activation of cathepsin C, which others have shown is involved in processing Leu-Leu-O-Me to its active, LMP-inducing form (Hornung *et al.*, 2008; Jacobson *et al.*, 2013; Brojatsch *et al.*, 2014). Therefore, Bafilomycin A1 inhibition of LMP with Leu-Leu-O-Me exposure may be due to less mature cathepsin C. It is important to note that Leu-Leu-O-Me as a detergent can act directly on lysosomes, whereas particles are taken into phagolysosomes and in this compartment membrane permeabilization occurs. Therefore, when referencing particle-induced LMP, rupture of the phagolysosome is inferred. Phagolysosome acidification has also been suggested to be required for silica-induced LMP based on findings in which NLRP3 inflammasome associated cytokine production was decreased following Bafilomycin A1 treatment in both silica and Leu-Leu-O-Me exposure models (Hornung *et al.*, 2008). However direct inhibition of silica-induced LMP with Bafilomycin A1 was not assessed in these reports, and could differ from Leu-Leu-O-Me due to it’s dependence on cathepsin C as discussed. While our results show a necessary role for acidification in particle-induced LMP consistent with alternative models of LMP (the use of Leu-Leu-O-

Me), they do not address mechanisms by which phagolysosome acidification enables particles to cause LMP. Lysosome acidification and activation of proteases has been reported to facilitate removal of the protein corona on phagocytosed particles, and thereby may allow for direct particle-membrane interactions (Wang *et al.*, 2013; Zhu *et al.*, 2016). Therefore, after the protein corona is removed, this would support the notion that specific physiochemical characteristics of the particle would define its LMP-inducing potential. This notion is supported by the fact that altering surface properties of silica and of multiple types of nanoparticles can have profound impacts on their relative toxicity (Morishige *et al.*, 2010; Sohaebuddin *et al.*, 2010; Hamilton *et al.*, 2013; Hamilton *et al.*, 2014; Pavan *et al.*, 2014; Peeters *et al.*, 2014). Alternatively, some studies have directly implicated cathepsin B in LMP (Werneburg *et al.*, 2002; Taha *et al.*, 2005; Jacobson *et al.*, 2013; Brojatsch *et al.*, 2014). We show that LMP occurs independent of cathepsin B and L with ENM exposure, as NAG levels in the cytosolic fraction were not reduced with CA-074-Me treatment (Figure 2, 5). Leaked NAG levels were partially reduced with silica exposure and CA-074-Me treatment (Figure 2B, 5B), suggesting a minor or indirect role for cathepsin B or L in LMP in this model. Particle-induced membrane damage via ROS has also been proposed as a mechanism of LMP (Boya and Kroemer, 2008; Domenech *et al.*, 2013). Nonetheless, mechanistic understandings of the contribution of these pathways (ROS and/or direct particle-membrane interactions) to initiating LMP have not been described.

All the particles utilized in these studies caused a dose-dependent increase in LMP (Figure 1A). However, we observed some significant differences in LMP kinetics between silica and ENM *in vitro* (Figure 1B), which could be due to multiple factors including mechanisms of uptake and differences in how much particle is initially taken up into phagolysosome compartments. Differences in the load of silica and ENM within the phagolysosome could greatly influence the amount and kinetics of phagolysosome acidification, cathepsin B activation, and consequently the level of NLRP3 inflammasome activity observed following LMP (Figure 2D, 2E), and in *ex vivo* AM cultures from particle-exposed mice at 7 d (Figure 6A, 6B, and 6G). Silica phagocytosis is mediated by MARCO (Biswas *et al.*, 2014), however, many of the uptake mechanisms of the ENM used in these studies have not been determined, but may include caveolin-1 or clatherin-mediated endocytosis (Kuhn *et al.*, 2014). The ENM used in these studies form larger agglomerates (Supplemental Table 1), which may be taken up through similar mechanisms to those utilized for micron-size silica. Specific physiochemical differences between the particles or particle agglomerates may influence the magnitude of membrane permeabilization that occurs following localization to the phagolysosome. Because of these differences, it is difficult to directly compare ENM to silica without further dosimetry evaluation, assessment of uptake mechanisms, intra-phagolysosome particle quantification, and manipulation of particle physiochemical characteristics, as well as time course studies on particle clearance. Regardless, all particles assessed in these studies caused LMP within 18 hr, consistent with the hypothesis that lysosome membrane permeabilization is the critical pathway following phagocytosis leading to NLRP3 inflammasome activation.

In vivo studies supporting LMP are lacking (Appelqvist *et al.*, 2013). There are multiple reports of LMP *in vitro* with a broad range of agonists but only a small number of reports showing an *in vivo* role for LMP (Kreuzaler *et al.*, 2011; Li *et al.*, 2016). Consequently, little

is known on the contribution of LMP to NLRP3 associated inflammation beyond what is observed *in vitro*. Ongoing LMP, including the leak of active cathepsins into the cytosol, may drive persistent NLRP3 inflammasome activity. Our observation of increased NLRP3 inflammasome activity at 7 d in isolated alveolar macrophages correlated with loss of lysosomal staining, and greater intracellular cathepsin B activity (Figures 4B, 4C, 4D, and 4E), consistent with an altered lysosome state. The altered lysosome state included LMP, which was evident in isolated AM following silica and ENM exposure *in vivo* (Figure 5). Both LMP and NLRP3 inflammasome activity in AM was mitigated *ex vivo* with Bafilomycin A1 and CA-074-Me treatment with silica exposure (Figure 5A, 5B, 6A, 6B). Cytosolic cathepsin activity is known to cause NLRP3 inflammasome activation *in vitro*, and therefore the therapeutic effects of CA-074-Me in AM *ex vivo* is likely due to inhibition of cytosolic cathepsin B and L resulting from ongoing LMP. Importantly, we show that cathepsin B and L activity are important components driving ongoing NLRP3 inflammasome activity in isolated lung macrophages in a model of murine silicosis (Figure 6D, 6E). The specific roles of each of these cathepsins were not determined in these studies and more specific gene targeting approaches will be required in the future to determine their respective contributions. However, the current study supports the hypothesis that that following LMP, cytosolic cathepsins are directly involved in driving the persistence of NLRP3 inflammasome activity. Further, these data support the possibility therapeutically targeting these pathways to diminish the inflammation that drives chronic disease.

Our observation of bimodal lysosome staining in lung lavage cells isolated from silica-exposed mice (Figure 4C) suggests the potential of LMP in a subset of lung macrophages. It is important to note that cathepsin B and lysosome-staining studies highlighted in Figure 4 measured averages of the entire population of cells isolated from the lung lavage fluid. Though most of the cells isolated are macrophages 7 d following silica exposure, these macrophages are not naïve, but likely consist of mixed phenotypes. Lysosome loss in a subset of macrophages that are expressing high levels of cathepsin B could define a subset of macrophages in which there is NLRP3 inflammasome hyperactivity or lysosome instability. The contribution of LMP and altered lysosomal activity within specific lung cell populations and/or macrophage subsets were not defined in these studies, but highlight important future directions.

HMGB1 is a Danger Associated Molecular Pattern/alarmin that is released by dead or dying cells, and can be actively secreted by macrophages (Gardella *et al.*, 2002; Willingham *et al.*, 2009). Once outside of the cell, HMGB1 may have both pro-inflammatory and/or chemotactic activity (Yang *et al.*, 2012; Tsung *et al.*, 2014). Both HMGB1 and IL-18 have been implicated in autoimmune diseases such as SLE, which has increased prevalence in individuals with silicosis (Dinarello, 2007; Leung *et al.*, 2012; Lu *et al.*, 2015). We have previously reported that HMGB1 participates in sterile priming of the NLRP3 inflammasome *in vitro* and *in vivo* with MWCNT exposure (Jessop and Holian, 2015). While we did not investigate the contribution of HMGB1 in priming NLRP3 inflammasome activity with silica exposure, we suspect commonality with MWCNT due to the analogous pathway of LMP and NLRP3 inflammasome activation. HMGB1 release has also been reported to be dependent upon NLRP3 inflammasome activation with endotoxemia, ATP, and nigericin exposure (Lamkanfi *et al.*, 2010). However, HMGB1 release was not decreased

with CA-074-Me treatment in their injury models. Our results show that HMGB1 secretion is dependent upon Caspase-1 and also cathepsin B/L with silica and ENM exposure, suggesting a potential role for LMP or lysosome activity (Figure 3D, 6C, 6G). Whether HMGB1 release is due to cell death resulting from LMP and NLRP3 inflammasome activity, or through an active secretion pathway, was not investigated in these studies. An autophagy-based unconventional secretion pathway for HMGB1 and NLRP3 inflammasome cytokines has been reported in models in which nigericin was used as the NLRP3 inflammasome agonist (Dupont *et al.*, 2011). We have recently reported that HMGB1 release is enhanced in autophagy deficient mice exposed to silica, likely through greater cell death (Jessop *et al.*, 2016). Likewise, the observation that elevated LDH and HMGB1 were both evident 7 d following silica exposure would suggest an association with increased cytotoxicity (Figure 6C, Supplementary Figure 5).

In summary, this study demonstrates several novel findings that further our understanding of particle-induced LMP and mechanisms driving persistent NLRP3 inflammasome activity. The central findings support a unifying principle that LMP is a central mechanism of particle-induced inflammation and toxicity (Bunderson-Schelvan *et al.*, 2016), and supports an integral role for phagolysosome acidification in licensing silica and ENM to cause LMP. Targeting LMP and or active cathepsins may provide a viable therapeutic approach for reducing particle-associated inflammation.

Supplementary Material

Refer to Web version on PubMed Central for supplementary material.

Acknowledgments

This work was support by a research grant from NIEHS (R01ES023209), Institutional Idea Award from NIGMS (P30 GM103338), and a S10 Shared instrument grant (S10RR026325–01). Additionally, Forrest Jessop was supported in part by a PhRMA Foundation Individual Pre-doctoral Fellowship. The content of this manuscript is solely the responsibility of the authors and does not necessarily represent the views of the National Institute of Health or the PhRMA Foundation. The authors are grateful for the technical support obtained through the CEHS Molecular Histology and Fluorescence Imaging, Inhalation and Pulmonary Physiology Cores, and Fluorescence Cytometry Core facilities. We extend a special thanks to the technical staff of these cores including Pam Shaw, Britt Postma, Mary Buford, and Lou Herritt. The authors thank Dr. John Hoidal, Dr. Christopher T. Migliaccio and Kevin Trout for scientific advice.

REFERENCES

Aits S, Jaattela M, Nylandsted J. Methods for the quantification of lysosomal membrane permeabilization: a hallmark of lysosomal cell death. Methods Cell Biol. 2015; 126:261–285. [PubMed: 25665450]

Appelqvist H, Waster P, Kagedal K, Ollinger K. The lysosome: from waste bag to potential therapeutic target. Journal of molecular cell biology. 2013; 5:214–226. [PubMed: 23918283]

Beamer CA, Migliaccio CT, Jessop F, Trapkus M, Yuan D, Holian A. Innate immune processes are sufficient for driving silicosis in mice. Journal of leukocyte biology. 2010; 88:547–557. [PubMed: 20576854]

Biswas R, Hamilton RF Jr, Holian A. Role of lysosomes in silica-induced inflammasome activation and inflammation in absence of MARCO. J Immunol Res. 2014; 2014:304180. [PubMed: 25054161]

Boya P, Kroemer G. Lysosomal membrane permeabilization in cell death. Oncogene. 2008; 27:6434–6451. [PubMed: 18955971]

Brojatsch J, Lima H, Kar AK, Jacobson LS, Muehlbauer SM, Chandran K, Diaz-Griffero F. A proteolytic cascade controls lysosome rupture and necrotic cell death mediated by lysosome-destabilizing adjuvants. PLoS One. 2014; 9:e95032. [PubMed: 24893007]

Bunderson-Schelvan, M., Hamilton, R., Trout, K., Jessop, F., Gulumian, M., Holian, A. Approaching a unified theory for particle-induced inflammation. In: Otsuki, T.Yoshioka, Yasuo, Holian, Andrij, editors. Biological Effects Of Fibrous And Particulate Substances. Japan: Springer; 2016. p. 51-76.

Buttle DJ, Murata M, Knight CG, Barrett AJ. CA074 methyl ester: a proinhibitor for intracellular cathepsin B. Arch Biochem Biophys. 1992; 299:377–380. [PubMed: 1444478]

Cassel SL, Eisenbarth SC, Iyer SS, Sadler JJ, Colegio OR, Tephly LA, Carter AB, Rothman PB, Flavell RA, Sutterwala FS. The Nalp3 inflammasome is essential for the development of silicosis. Proceedings of the National Academy of Sciences of the United States of America. 2008; 105:9035–9040. [PubMed: 18577586]

Dinarello CA. Interleukin-8 and the pathogenesis of inflammatory diseases. Semin Nephrol. 2007; 27:98–114. [PubMed: 17336692]

Domenech M, Marrero-Berrios I, Torres-Lugo M, Rinaldi C. Lysosomal membrane permeabilization by targeted magnetic nanoparticles in alternating magnetic fields. ACS nano. 2013; 7:5091–5101. [PubMed: 23705969]

Dostert C, Petrilli V, Van Bruggen R, Steele C, Mossman BT, Tschopp J. Innate immune activation through Nalp3 inflammasome sensing of asbestos and silica. Science. 2008; 320:674–677. [PubMed: 18403674]

Duewell P, Kono H, Rayner KJ, Sirois CM, Vladimer G, Bauernfeind FG, Abela GS, Franchi L, Nunez G, Schnurr M, Espevik T, Lien E, Fitzgerald KA, Rock KL, Moore KJ, Wright SD, Hornung V, Latz E. NLRP3 inflammasomes are required for atherogenesis and activated by cholesterol crystals. Nature. 2010; 464:1357–1361. [PubMed: 20428172]

Dupont N, Jiang S, Pilli M, Ornatowski W, Bhattacharya D, Deretic V. Autophagy-based unconventional secretory pathway for extracellular delivery of IL-1beta. The EMBO journal. 2011; 30:4701–4711. [PubMed: 22068051]

Gardella S, Andrei C, Ferrera D, Lotti LV, Torrisi MR, Bianchi ME, Rubartelli A. The nuclear protein HMGB1 is secreted by monocytes via a non-classical, vesicle-mediated secretory pathway. EMBO Rep. 2002; 3:995–1001. [PubMed: 12231511]

Gilberti RM, Joshi GN, Knecht DA. The phagocytosis of crystalline silica particles by macrophages. American journal of respiratory cell and molecular biology. 2008; 39:619–627. [PubMed: 18556590]

Girtsman TA, Beamer CA, Wu N, Buford M, Holian A. IL-1R signalling is critical for regulation of multi-walled carbon nanotubes-induced acute lung inflammation in C57Bl/6 mice. Nanotoxicology. 2014; 8:17–27. [PubMed: 23094697]

Hamilton RF Jr, Buford M, Xiang C, Wu N, Holian A. NLRP3 inflammasome activation in murine alveolar macrophages and related lung pathology is associated with MWCNT nickel contamination. Inhalation toxicology. 2012; 24:995–1008. [PubMed: 23216160]

Hamilton RF Jr, Thakur SA, Mayfair JK, Holian A. MARCO mediates silica uptake and toxicity in alveolar macrophages from C57BL/6 mice. The Journal of biological chemistry. 2006; 281:34218–34226. [PubMed: 16984918]

Hamilton RF Jr, Wu Z, Mitra S, Shaw PK, Holian A. Effect of MWCNT size, carboxylation, and purification on in vitro and in vivo toxicity, inflammation and lung pathology. Particle and fibre toxicology. 2013; 10:57. [PubMed: 24225053]

Hamilton RF, Wu N, Porter D, Buford M, Wolfarth M, Holian A. Particle length-dependent titanium dioxide nanomaterials toxicity and bioactivity. Particle and fibre toxicology. 2009; 6:35. [PubMed: 20043844]

Hamilton RF, Wu N, Xiang C, Li M, Yang F, Wolfarth M, Porter DW, Holian A. Synthesis, characterization, and bioactivity of carboxylic acid-functionalized titanium dioxide nanobelts. Particle and fibre toxicology. 2014; 11:43. [PubMed: 25179214]

Hornung V, Bauernfeind F, Halle A, Samstad EO, Kono H, Rock KL, Fitzgerald KA, Latz E. Silica crystals and aluminum salts activate the NALP3 inflammasome through phagosomal destabilization. Nature immunology. 2008; 9:847–856. [PubMed: 18604214]

Hughes CS, Colhoun LM, Bains BK, Kilgour JD, Burden RE, Burrows JF, Lavelle EC, Gilmore BF, Scott CJ. Extracellular cathepsin S and intracellular caspase 1 activation are surrogate biomarkers of particulate-induced lysosomal disruption in macrophages. Particle and fibre toxicology. 2016; 13:19. [PubMed: 27108091]

Jacobson LS, Lima H Jr, Goldberg MF, Gocheva V, Tsiperson V, Sutterwala FS, Joyce JA, Gapp BV, Blomen VA, Chandran K, Brummelkamp TR, Diaz-Griffero F, Brojatsch J. Cathepsin-mediated necrosis controls the adaptive immune response by Th2 (T helper type 2)-associated adjuvants. The Journal of biological chemistry. 2013; 288:7481–7491. [PubMed: 23297415]

Jessop F, Hamilton RF, Rhoderick JF, Shaw PK, Holian A. Autophagy deficiency in macrophages enhances NLRP3 inflammasome activity and chronic lung disease following silica exposure. Toxicol Appl Pharmacol. 2016; 309:101–110. [PubMed: 27594529]

Jessop F, Holian A. Extracellular HMGB1 regulates multi-walled carbon nanotube-induced inflammation in vivo. Nanotoxicology. 2015; 9:365–372. [PubMed: 24983895]

Kreuzaler PA, Staniszewska AD, Li W, Omidvar N, Kedjouar B, Turkson J, Poli V, Flavell RA, Clarkson RW, Watson CJ. Stat3 controls lysosomal-mediated cell death in vivo. Nat Cell Biol. 2011; 13:303–309. [PubMed: 21336304]

Kuhn DA, Vanhecke D, Michen B, Blank F, Gehr P, Petri-Fink A, Rothen-Rutishauser B. Different endocytotic uptake mechanisms for nanoparticles in epithelial cells and macrophages. Beilstein J Nanotechnol. 2014; 5:1625–1636. [PubMed: 25383275]

Lacher SE, Johnson C, Jessop F, Holian A, Migliaccio CT. Murine pulmonary inflammation model: a comparative study of anesthesia and instillation methods. Inhalation toxicology. 2010; 22:77–83. [PubMed: 20017595]

Lamkanfi M, Sarkar A, Vande Walle L, Vitari AC, Amer AO, Wewers MD, Tracey KJ, Kanneganti TD, Dixit VM. Inflammasome-dependent release of the alarmin HMGB1 in endotoxemia. J Immunol. 2010; 185:4385–4392. [PubMed: 20802146]

Lennon-Dumenil AM, Bakker AH, Maehr R, Fiebiger E, Overkleeft HS, Rosemblatt M, Ploegh HL, Lagaudriere-Gesbert C. Analysis of protease activity in live antigen-presenting cells shows regulation of the phagosomal proteolytic contents during dendritic cell activation. The Journal of experimental medicine. 2002; 196:529–540. [PubMed: 12186844]

Leung CC, Yu IT, Chen W. Silicosis. Lancet. 2012; 379:2008–2018. [PubMed: 22534002]

Li L, Niu H, Sun B, Xiao Y, Li W, Yuan H, Lou H. Riccardin D-N induces lysosomal membrane permeabilization by inhibiting acid sphingomyelinase and interfering with sphingomyelin metabolism in vivo. Toxicol Appl Pharmacol. 2016; 310:175–184. [PubMed: 27660101]

Lu M, Yu S, Xu W, Gao B, Xiong S. HMGB1 Promotes Systemic Lupus Erythematosus by Enhancing Macrophage Inflammatory Response. J Immunol Res. 2015; 2015:946748. [PubMed: 26078984]

Meunier E, Coste A, Olagnier D, Authier H, Lefevre L, Dardenne C, Bernad J, Beraud M, Flahaut E, Pipy B. Double-walled carbon nanotubes trigger IL-1beta release in human monocytes through Nlrp3 inflammasome activation. Nanomedicine. 2012; 8:987–995. [PubMed: 22100755]

Moles A, Tarrats N, Fernandez-Checa JC, Mari M. Cathepsin B overexpression due to acid sphingomyelinase ablation promotes liver fibrosis in Niemann-Pick disease. The Journal of biological chemistry. 2012; 287:1178–1188. [PubMed: 22102288]

Morishige T, Yoshioka Y, Inakura H, Tanabe A, Yao X, Narimatsu S, Monobe Y, Imazawa T, Tsunoda S, Tsutsumi Y, Mukai Y, Okada N, Nakagawa S. The effect of surface modification of amorphous silica particles on NLRP3 inflammasome mediated IL-1beta production, ROS production and endosomal rupture. Biomaterials. 2010; 31:6833–6842. [PubMed: 20561679]

Netea MG, van de Veerdonk FL, van der Meer JW, Dinarello CA, Joosten LA. Inflammasome-independent regulation of IL-1-family cytokines. Annu Rev Immunol. 2015; 33:49–77. [PubMed: 25493334]

Palomaki J, Valimaki E, Sund J, Vippola M, Clausen PA, Jensen KA, Savolainen K, Matikainen S, Alenius H. Long, needle-like carbon nanotubes and asbestos activate the NLRP3 inflammasome through a similar mechanism. ACS nano. 2011; 5:6861–6870. [PubMed: 21800904]

Pavan C, Rabolli V, Tomatis M, Fubini B, Lison D. Why does the hemolytic activity of silica predict its pro-inflammatory activity? Particle and fibre toxicology. 2014; 11:76. [PubMed: 25522817]

Peeters PM, Eurlings IM, Perkins TN, Wouters EF, Schins RP, Borm PJ, Drommer W, Reynaert NL, Albrecht C. Silica-induced NLRP3 inflammasome activation in vitro and in rat lungs. Particle and fibre toxicology. 2014; 11:58. [PubMed: 25406505]

Porter DW, Wu N, Hubbs AF, Mercer RR, Funk K, Meng F, Li J, Wolfarth MG, Battelli L, Friend S, Andrew M, Hamilton R Jr, Sriram K, Yang F, Castranova V, Holian A. Differential mouse pulmonary dose and time course responses to titanium dioxide nanospheres and nanobelts. Toxicol Sci. 2013; 131:179–193. [PubMed: 22956629]

Sager TM, Wolfarth MW, Andrew M, Hubbs A, Friend S, Chen TH, Porter DW, Wu N, Yang F, Hamilton RF, Holian A. Effect of multi-walled carbon nanotube surface modification on bioactivity in the C57BL/6 mouse model. Nanotoxicology. 2014; 8:317–327. [PubMed: 23432020]

Sohaebuddin SK, Thevenot PT, Baker D, Eaton JW, Tang L. Nanomaterial cytotoxicity is composition, size, and cell type dependent. Particle and fibre toxicology. 2010; 7:22. [PubMed: 20727197]

Solano-Lopez C, Zeidler-Erdely PC, Hubbs AF, Reynolds SH, Roberts JR, Taylor MD, Young SH, Castranova V, Antonini JM. Welding fume exposure and associated inflammatory and hyperplastic changes in the lungs of tumor susceptible a/j mice. Toxicol Pathol. 2006; 34:364–372. [PubMed: 16844664]

Stern ST, Adiseshaiah PP, Crist RM. Autophagy and lysosomal dysfunction as emerging mechanisms of nanomaterial toxicity. Particle and fibre toxicology. 2012; 9:20. [PubMed: 22697169]

Steverding D. The cathepsin B-selective inhibitors CA-074 and CA-074Me inactivate cathepsin L under reducing conditions. Open Enzyme Inhibition Journal. 2011; 4:11–16.

Taha TA, Kitatani K, Bielawski J, Cho W, Hannun YA, Obeid LM. Tumor necrosis factor induces the loss of sphingosine kinase-1 by a cathepsin B-dependent mechanism. The Journal of biological chemistry. 2005; 280:17196–17202. [PubMed: 15710602]

Tsung A, Tohme S, Billiar TR. High-mobility group box-1 in sterile inflammation. Journal of internal medicine. 2014; 276:425–443. [PubMed: 24935761]

Wang F, Yu L, Monopoli MP, Sandin P, Mahon E, Salvati A, Dawson KA. The biomolecular corona is retained during nanoparticle uptake and protects the cells from the damage induced by cationic nanoparticles until degraded in the lysosomes. Nanomedicine. 2013; 9:1159–1168. [PubMed: 23660460]

Werneburg NW, Guicciardi ME, Bronk SF, Gores GJ. Tumor necrosis factor-alpha-associated lysosomal permeabilization is cathepsin B dependent. Am J Physiol Gastrointest Liver Physiol. 2002; 283:G947–G956. [PubMed: 12223355]

Willingham SB, Allen IC, Bergstralh DT, Brickey WJ, Huang MT, Taxman DJ, Duncan JA, Ting JP. NLRP3 (NALP3, Cryopyrin) facilitates in vivo caspase-1 activation, necrosis, and HMGB1 release via inflammasome-dependent and -independent pathways. J Immunol. 2009; 183:2008–2015. [PubMed: 19587006]

Xia T, Hamilton RF, Bonner JC, Crandall ED, Elder A, Fazlollahi F, Girtsman TA, Kim K, Mitra S, Ntim SA, Orr G, Tagmount M, Taylor AJ, Telesca D, Tolic A, Vulpe CD, Walker AJ, Wang X, Witzmann FA, Wu N, Xie Y, Zink JI, Nel A, Holian A. Interlaboratory evaluation of in vitro cytotoxicity and inflammatory responses to engineered nanomaterials: the NIEHS Nano GO Consortium. Environmental health perspectives. 2013; 121:683–690. [PubMed: 23649538]

Yang H, Lundback P, Ottosson L, Erlandsson-Harris H, Venereau E, Bianchi ME, Al-Abed Y, Andersson U, Tracey KJ, Antoine DJ. Redox modification of cysteine residues regulates the cytokine activity of high mobility group box-1 (HMGB1). Mol Med. 2012; 18:250–259. [PubMed: 22105604]

Yoshimori T, Yamamoto A, Moriyama Y, Futai M, Tashiro Y. Bafilomycin A1, a specific inhibitor of vacuolar-type H(+)-ATPase, inhibits acidification and protein degradation in lysosomes of cultured cells. The Journal of biological chemistry. 1991; 266:17707–17712. [PubMed: 1832676]

Zhu W, von dem Bussche A, Yi X, Qiu Y, Wang Z, Weston P, Hurt RH, Kane AB, Gao H. Nanomechanical mechanism for lipid bilayer damage induced by carbon nanotubes confined in intracellular vesicles. Proceedings of the National Academy of Sciences of the United States of America. 2016; 113:12374–12379. [PubMed: 27791073]

Highlights

- Silica and nanoparticles cause LMP in macrophages *in vitro* and *in vivo*
- Phagolysosome acidification is required for particle-induced LMP
- Cathepsin B and L are not required for nanoparticle-induced LMP
- Cathepsin B/L regulate the secretion of HMGB1 with particle exposure

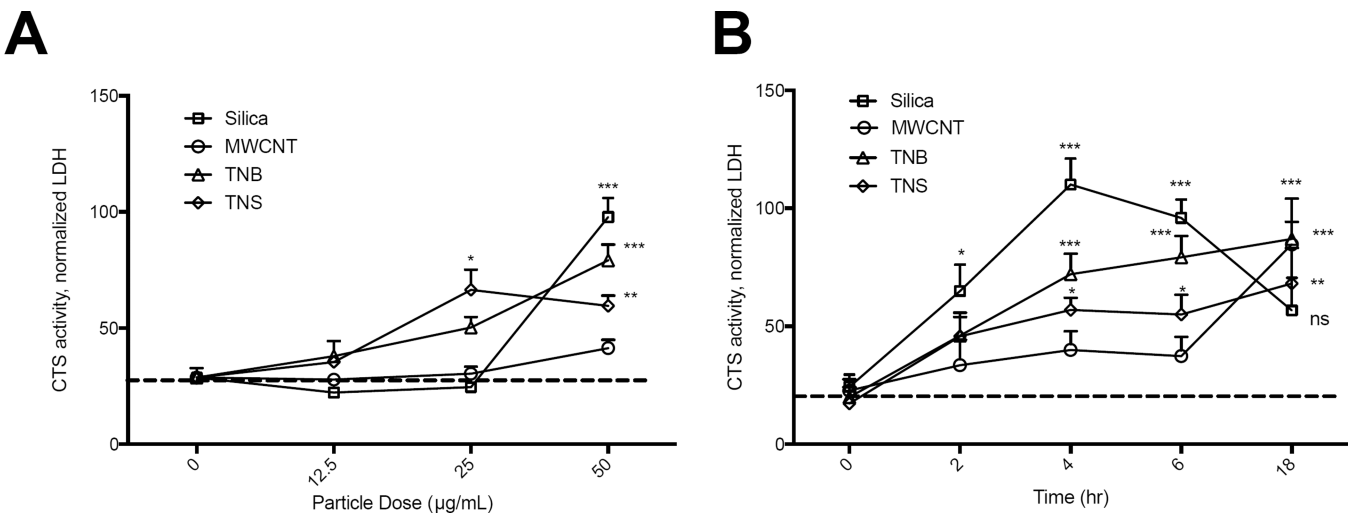

Figure 1. Silica and ENM exposure cause LMP in macrophages

(A) BMdM were exposed to increasing doses of silica, MWCNT, TNB, and TNS and LMP measured in the cytosolic fraction at 4 hr. (B) LMP over time with particle dose of 50 μg/mL. Data are presented as mean ± *SEM* (*N*=3). *P < 0.05, **P < 0.01, ***P < 0.001 when compared to baseline.

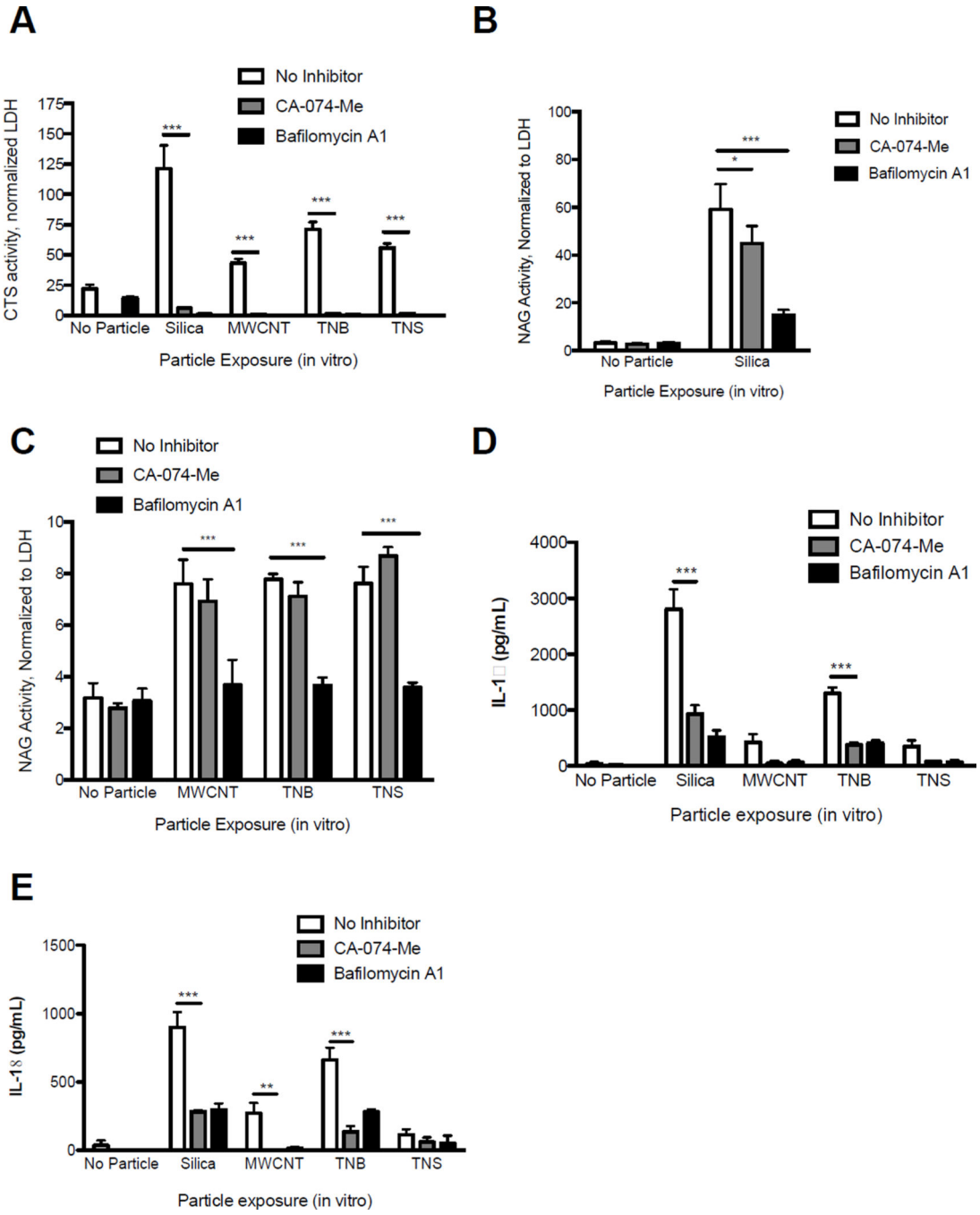

Figure 2. Particle-induced LMP in macrophages is dependent on phagolysosome acidification in vitro

BMdM were exposed to silica, MWCNT, TNB, or TNS (all 50 μg/mL) with or without Bafilomycin A1 (100 nM) or CA-074-Me (10 μM) and LMP assessed after 4 hr via digitonin extraction. (A) Cathepsin L activity in the cytosolic fraction. (B) NAG activity in the cytosolic fraction following silica exposure. (C) NAG activity in the cytosolic fraction following MWCNT, TNB, and TNS exposure. (D) IL-1β and (E) IL-18 levels in BMdM cell supernatants 24 hr after particle exposure with LPS stimulation (20 ng/mL) and treatment with Bafilomycin A1 (100 nM) or CA-074-Me (10 μM). Data show mean ± *SEM* (*N*=3). **P*

< 0.05, ** $P < 0.01$, *** $P < 0.001$ indicate significance compared to particle exposures without CA-074-Me or Bafilomycin A1 treatment.

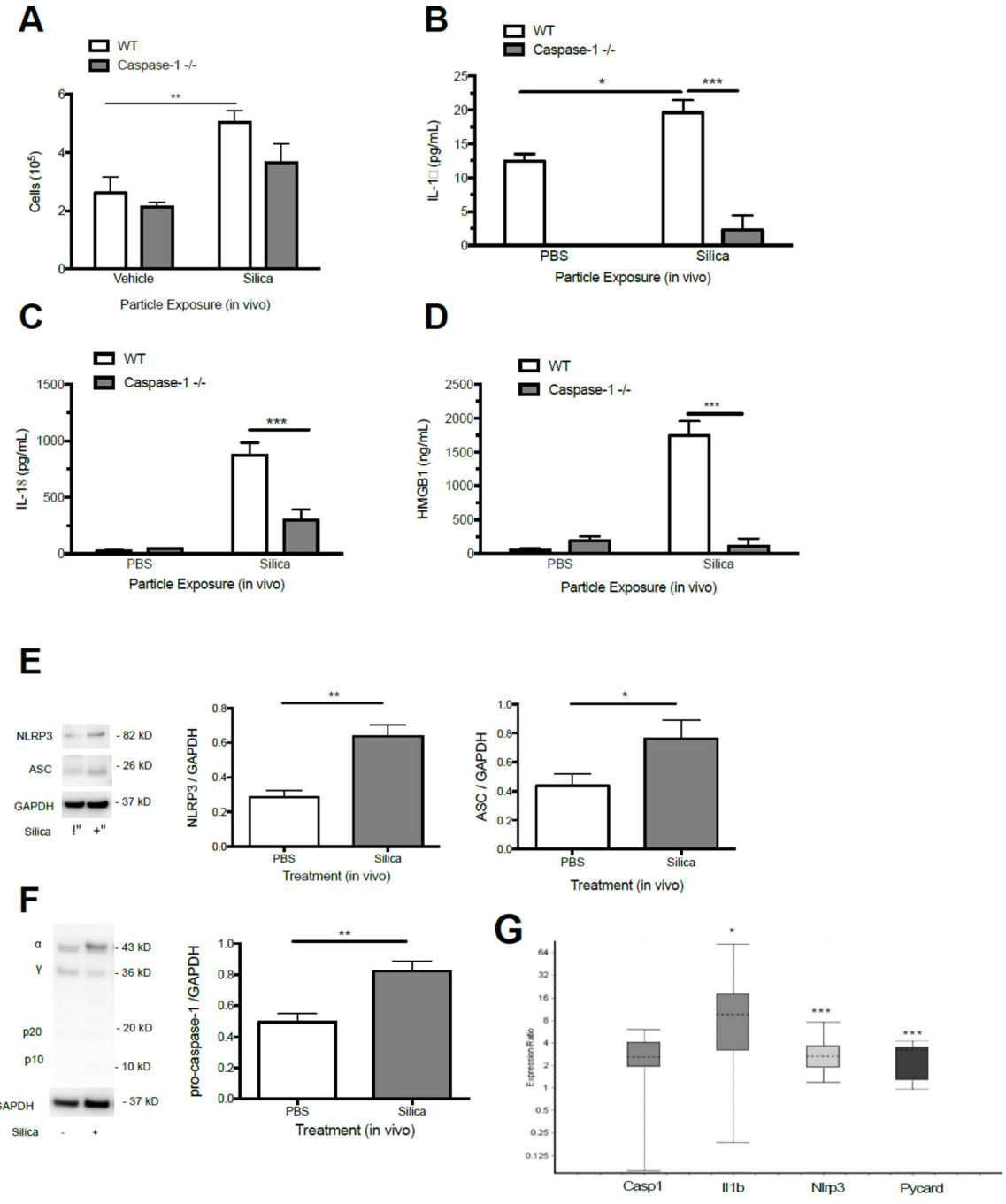

Figure 3. Silica exposure causes persistent NLRP3 inflammasome activity in vivo

(A) Total cell counts in the lavage fluid 7 d after silica (40 mg/kg) instillation in C57Bl/6 and caspase-1 null mice. (B) IL-1β, (C) IL-18, and (D) HMGB1 levels in the whole lavage fluid of C57Bl/6 and caspase-1 null mice at 7 d following instillation of PBS or silica (40 mg/kg). Data are presented as mean ± SEM (N=4). (E and F) Intracellular NLRP3, ASC, and pro-caspase-1 protein levels in isolated AM from C57Bl/6 mice 7 d following silica or PBS exposure. Western Blots shown are representative of 3 separate experiments with lung lavage cells from 3 mice pooled for each lysate. (G) mRNA expression in AM isolated from

C57Bl/6 mice 7 d following silica exposure relative to PBS control. Data shown as expression ratio with upper and lower quartiles and include 95% confidence intervals. *$P <$ 0.05, **$P < 0.01$, ***$P < 0.001$ indicates significance.

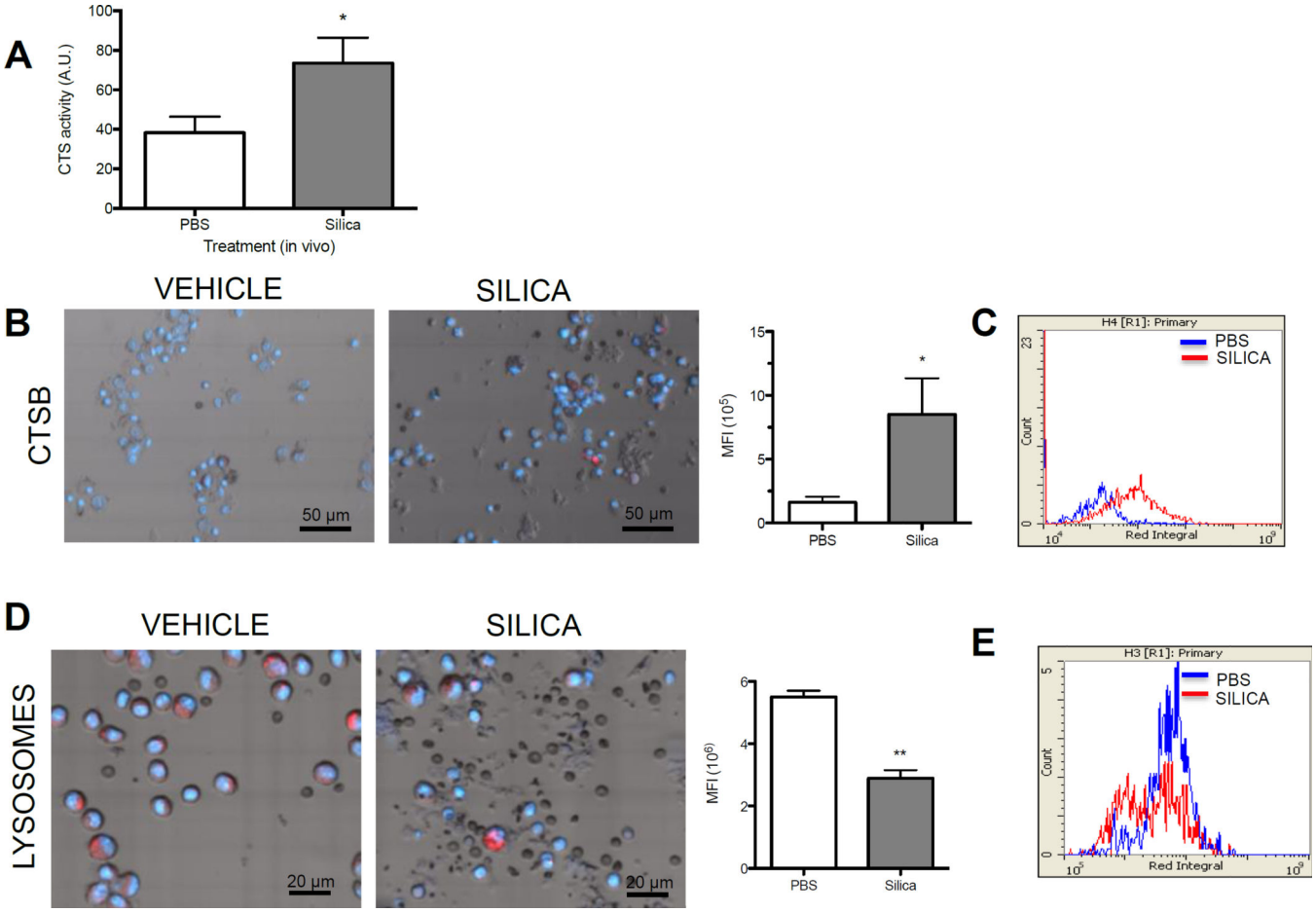

Figure 4. Silica exposure is associated with an altered lysosome staining in vivo

(A) Cathepsin activity in the whole lavage fluid of C57Bl/6 following instillation of PBS or silica (40 mg/kg) (N=4). (B) Representative LSC images (40X scan) and graph showing Mean Fluorescent Intensity (MFI per total cells counted) of cathepsin B in lung lavage cells isolated from PBS and silica exposed mice (N=4, 2 mice pooled for each N). (C) Histogram overlays of cathepsin activity substrate integrals from combined experiments. (D) Representative LSC images (60X scan) of Lysotracker Red™ staining with figure showing MFI of Lysotracker Red™ for combined experiments (N=4, 2 mice pooled for each N). (D) Histogram overlays of Lysotracker Red™ MFI integrals from combined experiments. Data are shown as mean ± SEM. *P < 0.05, **P < 0.01, ***P < 0.001 indicate significance.

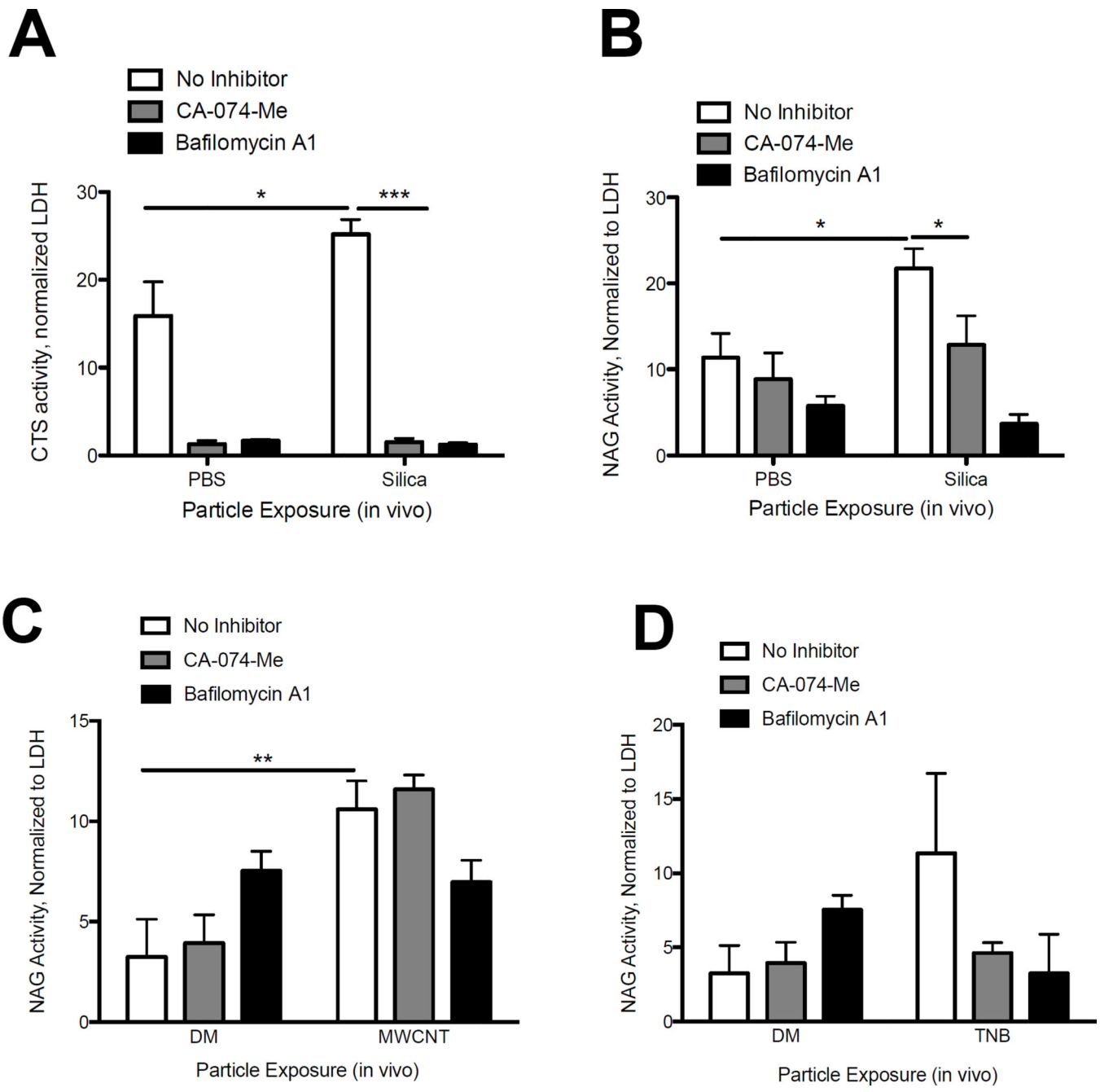

Figure 5. LMP is increased in AM 7 d following particle exposure in vivo

AM were isolated 7 d following silica (40 mg/kg) or PBS, TNB (2 mg/kg), MWCNT (2mg/kg), or dispersion media (DM) exposure and assessed for LMP via digitonin extraction. CA-074-Me (10 μM) or Bafilomycin A1 (100 nM) was added to AM *ex vivo* cultures for 2 hours. (A) Cathepsin L activity in cytosolic fraction of AM isolated from silica and PBS exposed mice. (B) NAG activity in the cytosolic fraction of AM isolated from silica and PBS exposed mice. (C) NAG activity in the cytosolic fraction of AM isolated from MWCNT and DM exposed mice. (D) NAG activity in the cytosolic fraction of AM isolated from TNB and

DM-exposed mice. Data are shown as mean ± *SEM*(*N*=4). **P* < 0.05, ***P* < 0.01, ****P* < 0.001 indicate significance.

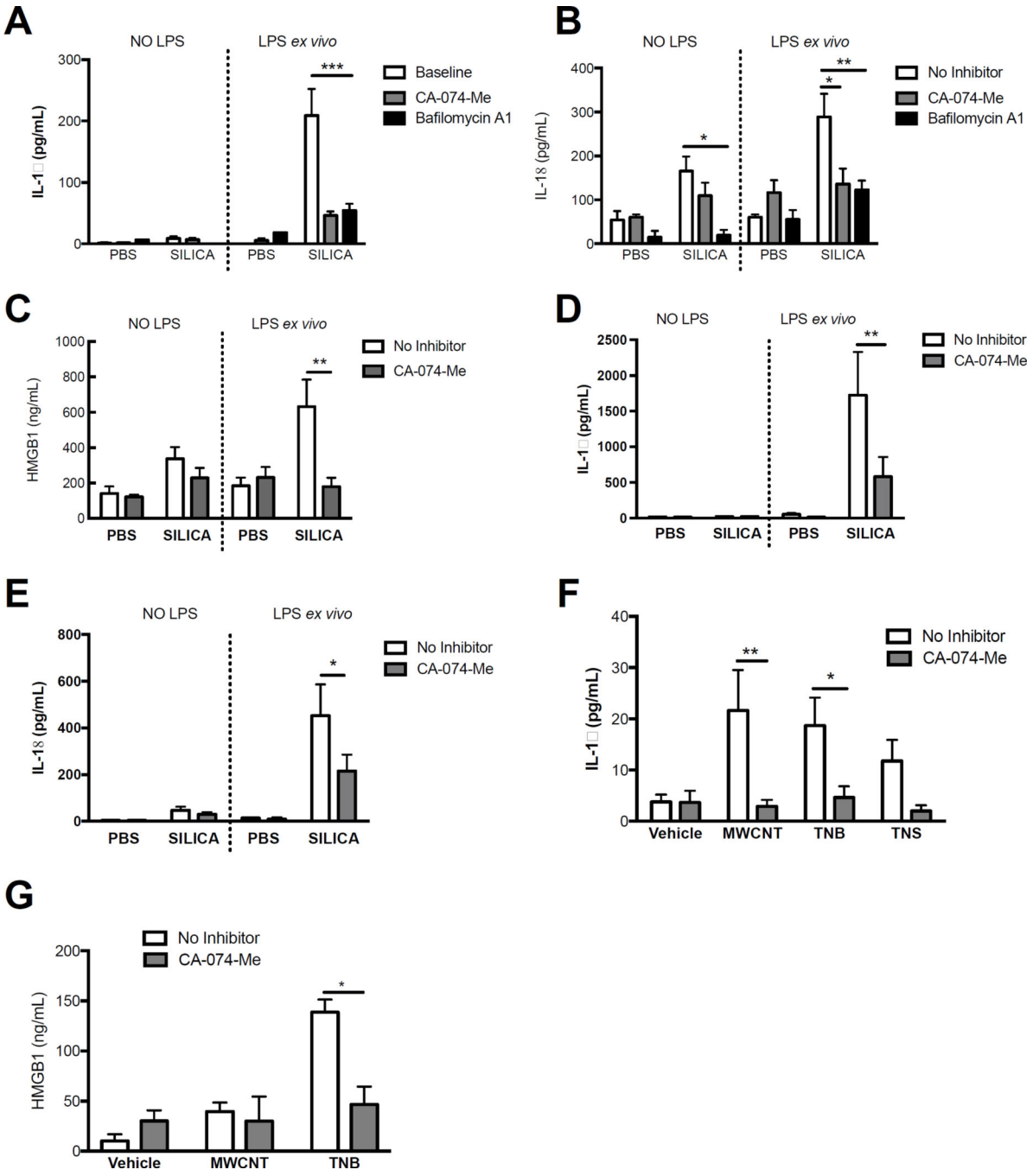

Figure 6. LMP and resultant cathepsin B activity drives persistent NLRP3 inflammasome activity in AM ex vivo following particle exposure

AM wereisolated from C57BL/6 mice 7 d following silica (40 mg/kg), MWCNT, TNB, and/or TNS (2 mg/kg) exposure and cultured *ex vivo* with/without LPS (20 ng/mL) stimulation and CA-074-Me (10 μM) or Bafilomycin A1 (100 nM) when designated in figure legend. Cytokine levels were measured in cell supernatants after 24 hr of *ex vivo* culture. (A) IL-1β levels in supernatants of AM cultured from silica or PBS exposed mice (7 d). (B) IL-18 levels in supernatants of AM cultured from silica or PBS exposed mice (7 d). (C) HMGB1 levels in cell supernatants after 24 hr from AM isolated and cultured from

silica or PBS exposed mice (7 d).(D) IL-1β levels in supernatants of AM cultured from silica or PBS exposed mice (56 d). (E) IL-18 levels in supernatants of AM cultured from silica or PBS exposed mice (56 d). (F) IL-1β levels in supernatants of AM from MWCNT, TNB, and TNS or vehicle exposed mice (7 d). (G) HMGB1 levels in supernatants of AM from MWCNT and TNB or vehicle-exposed mice (7 d, N=3). Data for all other experiments are shown as mean ± SEM (N=4). $*P < 0.05$. $**P < 0.01$. $***P < 0.001$ indicate significant reduction with inhibitor treatment.